

Effective Parameters on the Phase Morphology and Mechanical Properties of PP/PET/SEBS Ternary Polymer Blends

Mohammad Ali Khoramabadi¹, Omid Moini Jazani^{2,*}, Mohammad Mahdi Salehi³, Hossein Riazi⁴, Fariba Soltanolkottabi⁵

¹ Department of Polymer Engineering, College of Polymer Engineering, Mahshahr Branch, Islamic Azad University, Mahshahr, Iran.

² Department of Chemical Engineering, College of Engineering, University of Isfahan, Isfahan, Iran.

³ Polymer and Science Technology Division, Research Institute of Petroleum Industry (RIPI), Tehran, Iran.

⁴ Department of Polymer Engineering and Color Technology, Amirkabir University of Technology, Tehran, Iran.

⁵ Department of Engineering, Shahreza Branch, Islamic Azad University, Shahreza, Iran.

HIGHLIGHTS

- It was found that Dynamic Interfacial Energy prediction method is just able to prognosticate dominant morphology.
- The yield stress is controlled by several factors such as, volume fraction, average diameter and size distribution of the dispersed phases and also the interfacial between disperse and the matrix.
- With increasing the rubbery phase, the core-shell morphology and the impact strength increased while the modulus decreased.

ARTICLE INFO

Article history:

Received 20 November 2014

Received in revised form

12 December 2014

Accepted 14 December 2014

Keywords:

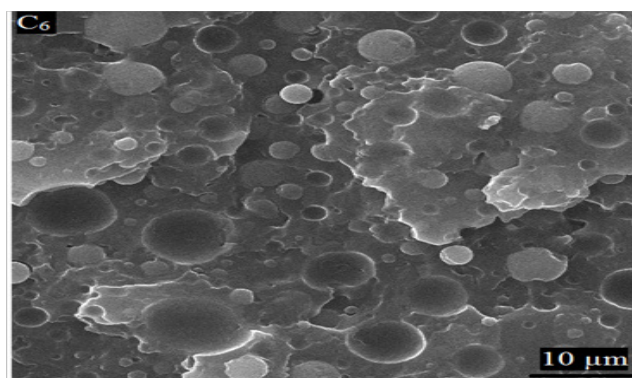
Ternary Blend

Morphology

Mechanical Properties

PP/PET/SEBS

GRAPHICAL ABSTRACT



ABSTRACT

In this work, ternary polymer blends based on polypropylene (PP)/ polyethylene terephthalate (PET) /poly(styrene-*b* (ethylene-co-butylene)-*b*-styrene) (SEBS) triblock copolymer and a reactive maleic anhydride grafted SEBS (SEBS-g-MAH) at various compositions were prepared by co-rotating twin screw extruder. The effects of PET, SEBS and SEBS-g-MAH compatibilizer on morphology of the blends were examined by scanning electron microscopy (SEM). The blends morphology was also estimated by some predicting methods, however, SEM results revealed some contrasts between results of predicting methods and the real morphology. Population of individual and core-shell particles as well as average diameter of the rubber-based cavities is extremely dependent on SEBS, SEBS-g-MA and PET content. Mechanical inspection tests showed that in comparison with the pure PP, addition of SEBS/SEBS-MA causes an increase in the impact strength of the system. Keeping other parameters constant, with increase in SEBS rubbery phase, the core-shell morphology was affected and the impact strength increased consequently. On the other hand, increase in PET content results in modulus increase and the impact strength decrease. Finally, the optimum processing conditions for compounding ternary PP/PET/SEBS blends were achieved.

*Corresponding author: o_moini@yahoo.com

1. Introduction

Polymer blending is a convenient and attractive route for obtaining new polymeric materials. Due to intricacy of the morphology and the mechanical properties of blended systems, researchers try to establish prediction rules to estimate final blend properties. In such systems, morphology directly affects final mechanical features. It is noteworthy to mention that morphology itself is determined by parameters like interfacial tension, components viscosity, composition ratio and processing conditions. Thus, it has been tried here to establish correlation between morphology and mechanical properties of blends considering such determining parameters.

Investigation of ternary polymer blends was first commenced in 1980 by Hobbs et al. [1] while studying morphology of blends consisting of three different phases. They observed that in some ternary systems one of the minor phases forms a layer around the other minor phase (core-shell morphology) but in some others the two minor phases separately disperse in the matrix of the major phase (separated dispersed morphology). They used Harkin's spreading coefficient concept to explain the effects of interfacial tension on phase morphology of different ternary blends. For a ternary system with A as the matrix phase and B and C as the dispersed phases, the spreading coefficient of the B-phase on the C-phase, λ_{BC} , and spreading coefficient of the C-phase on the B-phase, λ_{CB} , are estimated by following equations:

$$\lambda_{BC} = \gamma_{AC} - \gamma_{AB} - \gamma_{BC} \quad (1)$$

$$\lambda_{CB} = \gamma_{AB} - \gamma_{AC} - \gamma_{BC} \quad (2)$$

In the above-mentioned relations, γ_{ij} is the interfacial tension for each component pair. The positive value of λ_{BC} shows encapsulation of the C-phase by the B-phase while positive value of λ_{CB} signifies encapsulation of the B-phase by C-phase. In the Figure 1, four morphologies of a ternary system are presented which are the most stable ones as well.

Guo et al. [3] developed a new model to predict the morphology of ternary blends. They used a parameter named interfacial free energy that is originated from combination of interfacial tension and interfacial area. They presented three equations for different morphologies which are displayed in eq3-eq5:

$$(\sum A_i \gamma_{ij})_{B+C} = (4\pi)^{1/3} \left[n_B^{1/3} x^{2/3} \gamma_{AB} + n_C^{1/3} \gamma_{AC} \right] * (3V_C)^{2/3} \quad (3)$$

$$(\sum A_i \gamma_{ij})_{B/C} = (4\pi)^{1/3} \left[n_B^{1/3} (1+x)^{2/3} \gamma_{AB} + n_C^{1/3} \gamma_{BC} \right] * (3V_C)^{2/3} \quad (4)$$

$$(\sum A_i \gamma_{ij})_{C/B} = (4\pi)^{1/3} \left[n_B^{1/3} x^{2/3} \gamma_{BC} + n_C^{1/3} (1+X)^{2/3} \gamma_{AC} \right] * (3V_C)^{2/3} \quad (5)$$

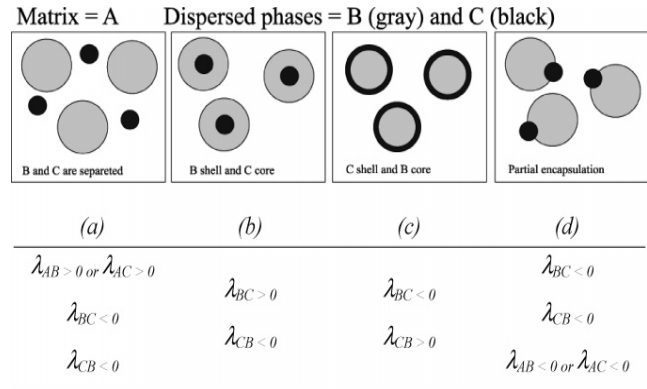


Fig. 1. Various stable morphologies of a ternary polymer blend [2].

In these equations, $x = V_B/V_C$ and V_i is the volume fraction of i phase. n_B and n_C are population of B-phase and C-phase particles, respectively. By assuming $n_B = n_C$, Guo et al. [3,4] calculated the interfacial energy for each phase structure in a simplified form as follows:

$$(RIE)_{B+C} = (\sum A_i \gamma_{ij})_{B+C} / K = X^{2/3} \gamma_{AB} + \gamma_{AC} \quad (6)$$

$$(RIE)_{B+C} = (\sum A_i \gamma_{ij})_{B+C} / K = X^{2/3} \gamma_{AB} + \gamma_{AC} \quad (7)$$

$$(RIE)_{B/C} = (\sum A_i \gamma_{ij})_{B/C} / K = (1+X)^{2/3} \gamma_{AB} + \gamma_{BC} \quad (8)$$

$$k = (4\pi)^{1/3} (n_c)^{1/3} (3V_c)^{2/3}, \quad x = V_B/V_C$$

Where $(RIE)_{B+C}$ is the relative interfacial energy of two minor components in a separately dispersed morphology, $(RIE)_{B/C}$ denotes to a morphology in which the B phase encapsulates C and $(RIE)_{C/B}$ shows the morphology in which the C phase encapsulates B.

Reignier et al. [5,6] introduced the dynamic interfacial tension terms into the minimum free energy theory of Guo et al. [3] by replacing the static interfacial tension. This led to following equations:

$$(\sum A_i \gamma_{ij})_{B+C} = 4\pi R_i^2 [\gamma_{AB} + R_i / 6(N_{1,B} - N_{1,A})] + 4\pi R_i^2 [\gamma_{AC} + R_i / 6(N_{1,B} - N_{1,A})] \quad (9)$$

$$(\sum A_i \gamma_{ij})_{C/B} = 4\pi R_e^2 [\gamma_{AC} + R_e / 6(N_{1,C} - N_{1,A})] + 4\pi R_i^2 [\gamma_{BC} + R_e / 6(N_{1,B} - N_{1,C})] \quad (10)$$

$$(\sum A_i \gamma_{ij})_{B/C} = 4\pi R_e^2 [\gamma_{AB} + R_e / 6(N_{1,B} - N_{1,A})] + 4\pi R_i^2 [\gamma_B + R_i / 6(N_{1,C} - N_{1,B})] \quad (11)$$

In these equations, N_1 is the first normal stress difference for A, B, and C phases, R_i and R_e are the internal

and the external radius of core-shell particles and γ_{ij} is the interfacial tension between components *i* and *j*.

These models including the spreading coefficient, the minimal free energy surface, the relative interfacial energy and the dynamic interfacial tension have been widely used by different researchers to predict the ternary blends morphology.[1-4, 6-10]

In the field of morphology and its correlation to the mechanical properties, many researchers have done extensive investigations. Jiang *et al.* studied POE (ethylene- α -olefin copolymer)/PS/SEBS system and showed that in comparison with the binary blends of the same system, addition of SEBS increases tensile strength. This improvement is attributed to formation of several network-like structures [11]. Ozcelik *et al.* also evaluated recycled PA6/ABS and PA6/PA66/ABS blends and found that increase in recycling steps leads to degradation of mechanical properties of the binary blends while improves mechanical properties of the ternary ones[12]. Han *et al.*[13] evaluated influence of blend composition on the mechanical properties and morphology of PC/ASA (acrylonitrile-styrene-acrylic terpolymer)/SAN ternary blends. Addition of SAN into PC/ASA blends improves the rubber dispersion efficiency and consequently results in higher impact strength. Vranjes *et al.*[14] studied the ternary polymer blends based on PP/EPDM/HDPE showing as morphology of the blends approaches to finer ones, the mechanical properties move toward superior states. Moïni *et al.*[15] evaluated the mechanical properties of PP/PC/SEBS ternary polymer blends using the Taguchi experimental analysis. They found that the optimum processing conditions leading to high impact strength, acceptable Young's modulus, and suitable yield stress are achievable at temperature equals to 255 °C, screw rotation speed of 130 rpm. The appropriate addition sequence was also pre-blending of PP and SEBS-g-MAH and then extruding it with PC and SEBS. Zhou *et al.* investigated PP/EPDM/HDPE blend using two different grades of EPDM with various viscosity. Application of lower-viscosity EPDM resulted in significant improvement in impact strength which is attributed to formation of appropriate core-shell structures [16].

Li *et al.*[17] studied the influences of component ratio of the minor phases on morphology and mechanical properties of ternary blends based on PP/PS/PA6. They concluded that the morphology state is independent of disperse phases ratio and just depends on the spreading coefficient concept. Moreover, when PA6 encapsulated PS phase, the blend showed better tensile strength and flexural strength which is attributed to improved adhesion between the phases. Wang *et al.*[18]

studied the ternary blends based on PA6/POE-g-MAH/EVOH in which addition of POE-g-MAH (the elastomeric phase) resulted in fourteen times increase in the impact strength. It was also deduced that tensile strength increases with increasing loading percentage of EVOH. D.H.Park *et al.*[19] evaluated the effects of compatibilizers on the mechanical properties of ternary polymer blends based on PP/EPDM/PLA(Poly Lactic acid). In the research, they used PP-g-MA and SEBS-g-MA as compatibilizers. Under such circumstances, PP-g-MA increases the tensile strength and SEBS-g-MA increases the impact strength while reducing the tensile strength. However, when both compatibilizers are used simultaneously, significant increase in the impact strength of the blend without any loss of tensile strength was obtained. Moïni *et al.* [20] studied PP/PTT/SEBS system and found that absence of compatibilizer is associated with lowest impact strength while simultaneous usage of SEBS and SEBS-g-MA as compatibilizer results in highest impact strength. This is due to strength of PTT and toughness of SEBS. Zhang *et al.* [21] evaluated effects of the core-shell structure on two ternary blends including ASA (acrylonitrile-styrene-acrylic terpolymer)/SAN/ACR(Acrylic resin) and SAN/ASA/ACR. It was found that impact strength was enhanced with increase of ACR in ASA/SAN/ACR and SAN/ASA/ACR. Consequently, the elongation at break increased and the tensile strength decreased. This reduction of the tensile strength is mainly due to the lower strength and modulus of ACR.

In this study, we investigated the role of effective parameters on the phase morphology and mechanical properties of PP/PET/SEBS ternary blends. The formulations were such designed to understand optimum ratio of SEBS to SEBS-g-MAH. It was also tried to estimate morphology of the blends by some predicting rules and compare the results with real morphologies obtained from SEM. Finally, by varying amount of PET and SEBS-g-MAH, their effects on properties like impact strength and modulus was understood.

2. Experimental

2.1. Materials

The following materials were used in this research: (PP), Grade HP550J supplied by Jaam Petrochemical company-(Iran), (MFI: 3.2 g/10 min, 230 °C, 2.16 kg), Polyethylene terephthalate (PET) purchased from Shahid Tondgooian Petrochemical Co.(Mahshahr Iran), Pars grade PET-amorphous chips, (Intrinsic Viscosity 0.63±0.03 dl/g, Carboxyl End Group ≤40 meq/Kg, Melting Point 249±3 °C). Poly(styrene-*b*-(eth

ylene-co-butylene)-b-styrene) (SEBS) tri-block copolymer, Kraton TM G1652 supplied by Shell Chemicals (29% styrene; molecular weight styrene block 7000 and EB block 37500 gr/mol, MFI: 5 g/10 min, 5 kg, 230°C); Maleic-anhydride grafted SEBS (SEBS-g-MAH) tri-block copolymer, Kraton TM FG1901x supplied by Shell Chemicals (29% styrene, nominal weight of grafted maleic anhydride = $1.8 \pm 0.4\%$, MFI: 22 g/10 min, 5 kg, 230 °C). Cyclohexane was also purchased from Merck Co.

2.2. Blend preparation

In this study, three ternary blends of PP/PET/ mixed (SEBS+SEBS-g-MAH) were produced at different weight ratio of SEBS to SEBS-g-MAH (I_1 - I_3) and six blends were produced at different weight ratio of PET and SEBS (C_1 - C_3 weight ratio of PET and C_4 - C_6 weight ratio of SEBS changed), Table 1. Compounding was performed by a Brabender co-rotating twin screw extruder (diameter of screw = 2 cm, length/diameter ratio=40). Before processing, the materials were dried in an oven for at least 20 h at 100 °C. The barrel of extruder had six temperature-control zones and their temperatures were set at 230–235–240–245–250–255 °C (from hopper to die). PP and SEBS-g-MAH were first pre-blended and then extruded with PET and SEBS. The extrudates were quenched in a cooling water bath and pelletized in a granulator. The screw speed was maintained at 130 rpm.

Table 1.
Composition ratio of the ternary blends.

Sample	PP (wt %)	PET (wt %)	SEBS+SEBS-g-MA (wt %)	Weight ratio of SEBS to SEBS-g-MAH
I_1	70	15	15	100/0
I_2	70	15	15	50/50
I_3	70	15	15	0/100
C_1	81	9	10	50/50
C_2	72	8	20	50/50
C_3	63	7	30	50/50
C_4	81	10	9	50/50
C_5	72	20	8	50/50
C_6	63	30	7	50/50

2.3. Mechanical properties

The dried pelletized blends were molded to form tensile and impact specimens using an ENGEL injec-

tion molding machine. The barrel temperature profile was 180 °C (hopper) to 240 °C (nozzle) and the mold temperature was maintained at 40 °C. Tensile stress-strain data were obtained using a Shimadzu AG-IS-5KN testing machine with cross head speed of 50 mm/min according to the ASTM D-638. Moreover Izod impact strength was measured for notched specimens according to ASTM D-256 using a Toyoseiki DJ-IS tester.

2.4. Morphological studies

To evaluate the effects of particle size and the type of morphology on the mechanical properties of PP/PET/SEBS ternary blends, micrographs of scanning electron microscopy (SEM) were recorded using a TScan VEGA II through fracture surface of impact specimens. Before the SEM studies, the impact samples were fractured in liquid nitrogen and subsequently were etched by cyclohexane for 24 h to remove SEBS and SEBS-g-MAH minor phases. Then, the etched samples were gold sputtered to make the samples conductive. Also the ImageJ software was used for image analysis of the SEM micrographs. In ImageJ software, according to the following procedure, images were analyzed. First, the software calibrated according to the scale of the images (set scale). Second, the required measures that should be registered in output file of the image software were defined, the images were opened, and, according to the instruments, were started to analyze. The images of the samples consisted of individual particles, core-shell composite particles and cavities. Counting was performed visually. After counting, each part is marked to prevent from error and according to defined parameters at calibration stage, output was showed in an Excel file.

3. Results and discussion

3.1. Morphology

To study morphology and predict it, two methods including RIE [2,4] and Dynamic Interfacial Energy were applied [5]. The interfacial tension coefficients were obtained using harmonic mean equation [22] as:

$$\gamma_{ij} = \gamma_i + \gamma_j - \frac{4\gamma_i^d \gamma_j^d}{\gamma_i^d \gamma_j^d} - \frac{4\gamma_i^p \gamma_j^p}{\gamma_i^p \gamma_j^p} \quad (12)$$

Where γ_{ij} is the interfacial tension between compo-

nents i and j , is the surface tension of component i , γ_i^d and γ_i^p are also dispersive fraction and polar fraction of surface tension of the component i , respectively. For calculate γ_{ij} table 2 was used.

Table 2.
surface tension and its components for various polymers.

Polymer	$\gamma(mN\ m^{-1})$	$\gamma^d(mN\ m^{-1})$	$\gamma^p(mN\ m^{-1})$	$d\gamma/dT(mN\ m^{-1})$
PP	15.3	14.99	0.31	-0.065
PET	28.0	21.81	6.19	-0.058
r-EB	22.2	21.76	0.44	-0.045

For the RIE method, calculation accomplished with equations (6)-(8) while for the Dynamic Interfacial Energy method, equations (9)-(11) used. To better simulate real processing conditions, the first normal stress difference (N_1) was also considered in the latter method and calculated using the following equation^[5]:

$$N_1 = \psi_1 \dot{\gamma}^2 \quad (13)$$

That for ψ_1 the following equation was utilized^[5]:

$$\psi_1(\dot{\gamma}) = 2G/\omega_2 [1 + (G'/G'')^2]^{0.7} \quad (14)$$

where G' is storage module, G'' is loss module and ω is frequency rate. Moreover shear rate ($\dot{\gamma}$) for a twin screw extruder was calculated from following equation:

$$\dot{\gamma} = \pi DN/60H \quad (15)$$

where D is screw diameter, H is screw depth and N is screw speed. Finally, for the RIE and Dynamic Interfacial Energy methods, calculation completed and showed in table 3.

In these blends, PP is the major component which makes the continuous phase and SEBS and PET are

minor phases. In the above table, PET is shown by B component and SEBS is displayed by C. According to these models (RIE and Dynamic Interfacial Energy), B+C is a morphology in which two minor phases are separated from each other and are dispersed in the continuous phase. B/C is the morphology in which core-shell particles with C as core and B as shell are dispersed in the continuous phase. Finally, C/B is a system that contains core-shell particles with Core C and shell B which are dispersed in the continuous phase. The lowest amount between B+C, B/C and C/B denotes to the dominant morphology of the system. For example, the RIE method predicts presence of core-shell particles (PET as core and SEBS as shell) in the continuous phase of I_1 . The RIE method predicts the same trend for I_2 and I_3 as well. However, SEM micrographs revealed a disparity between prediction results and real morphologies.

In the Figure 2, SEM micrographs of I_1 , I_2 and I_3 are presented. The system not only includes core-shell particles, but also has individual PET and rubbery domains. For example, the region shown by symbol a in the image I_1 points out to an core-shell particle while region b shows a cavity and region c is an individual PET particle. Cavities are formed due to dissolution of rubbery phase (SEBS and SEBS-g-MAH) in cyclohexane. Thus, it is obvious that prediction methods are not able to estimate the blend morphology completely. The RIE and Dynamic Interfacial Energy methods predicted core-shell and separated fully dispersed morphologies for I_1 sample, respectively. However, rubber-based cavities, individual PET particles and core-shell ones exist simultaneously. In the Figure 3, micrographs of other samples are presented. Above-mentioned descriptions are also valid for these samples.

SEM micrographs were analyzed by ImageJ software to gain an in-depth insight into the morphologies. The results are presented in the Table 4.

Table 3.
Results of prediction of morphology of the ternary blends by RIE and dynamic interfacial energy methods.

SAMPLE	RIE			Dynamic	Interfacial	Energy
	C+B	C/B	B/C	C+B	C/B	B/C
I_1	6.52	5.82	14.436	1.80E+04	1.21E+05	-6.52E+04
I_2	9.67	8.66	16.92	1.26E+06	1.16E+06	1.29E+06
I_3	6.52	5.82	14.436	1.12E+06	5.75E+05	1.25E+06
C_1	9.05	8.1	16.42	6.12E+04	2.52E+05	1.32E+04
C_2	5.57	4.94	13.73	2.40E+05	9.35E+05	6.50E+04
C_3	4.43	3.93	12.96	7.49E+04	5.21E+05	-3.71E+04
C_4	10.224	9.174	13.64	1.31E+05	1.07E+05	1.20E+05
C_5	16.66	15.15	23.14	4.07E+05	2.85E+05	3.88E+05
C_6	23.3	21.38	29.37	2.30E+06	9.75E+03	2.76E+06

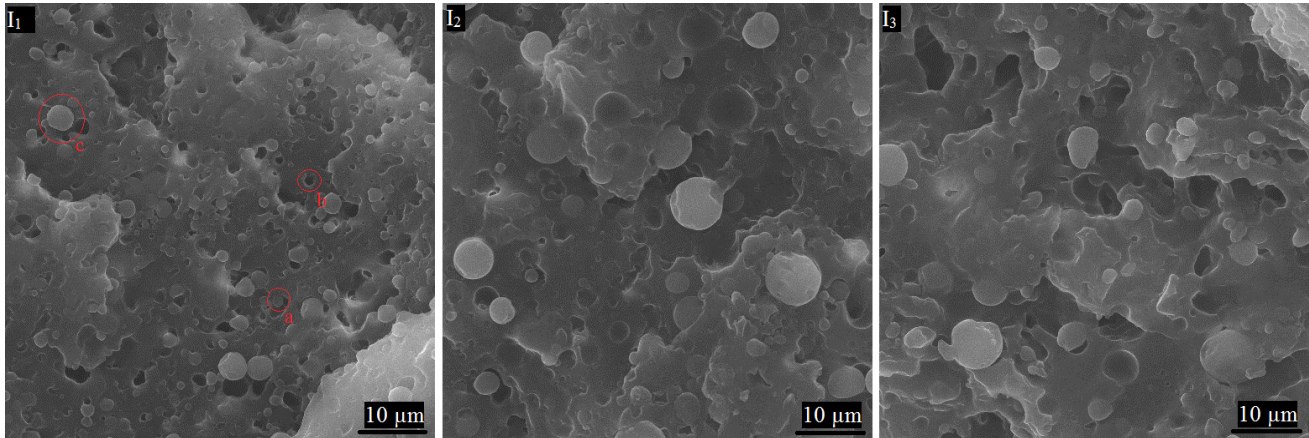


Fig. 2. SEM micrographs of I₁, I₂ and I₃ samples.

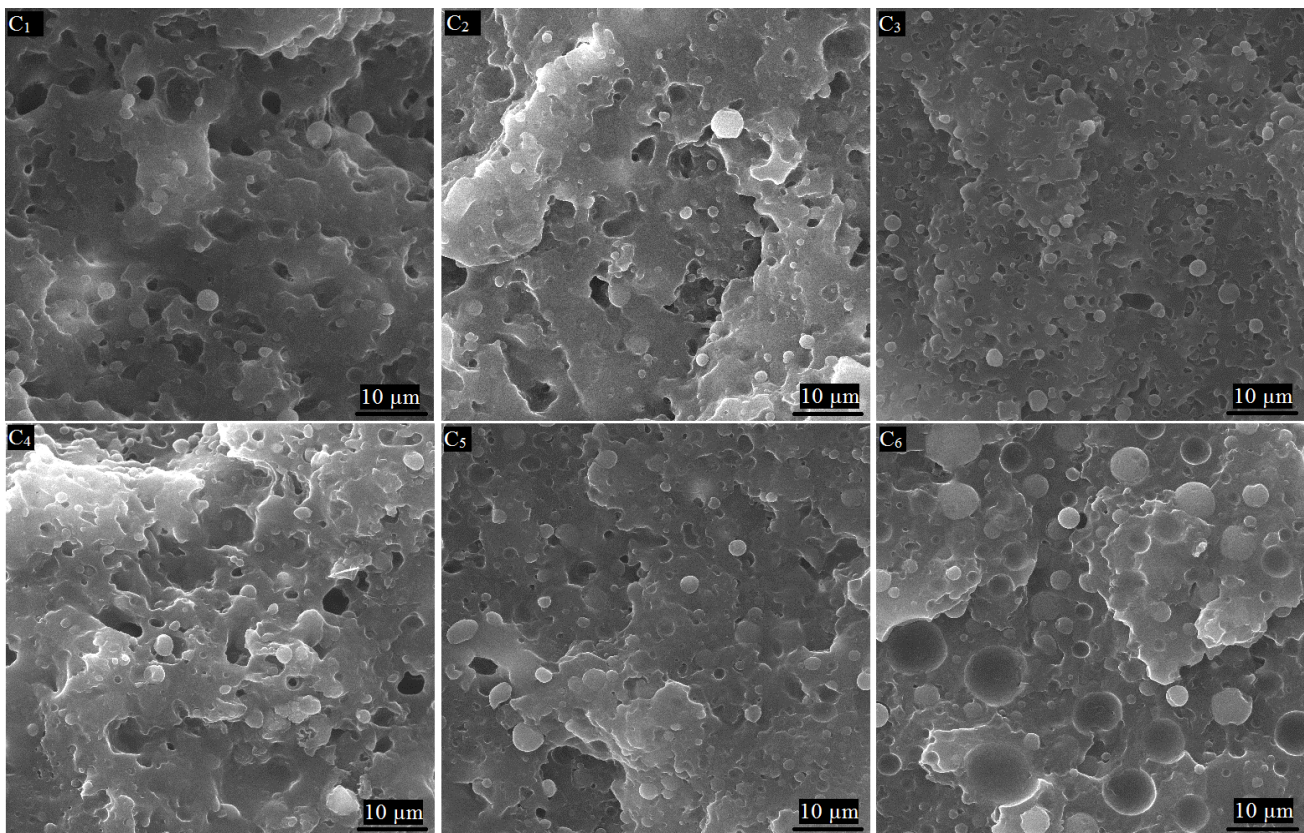


Fig. 3. SEM micrographs of C₁-C₆ samples.

Table 4.
Results of analysis of micrographs by ImageJ software.

Sample code	Number average diameter of cavity (μm)	Number of cavity	Number average diameter of individual particles (μm)	Number of individual particles	Number average diameter of composite droplets (μm)	Shell diameter(μm)	Number of composite droplets
I ₁	1.3549	93	1.56321	43	2.26875	0.712	14
I ₂	0.9497	11	3.53871	14	3.441143	0.683	20
I ₃	1.8564	24	2.01936	11	3.122667	0.473	9
C ₁	0.9356	47	1.27785	40	1.640679	0.635	13
C ₂	1.8715	22	1.59171	28	2.004333	0.927	17
C ₃	2.5219	20	1.46493	21	2.553	0.968	29
C ₄	1.906	69	1.95669	107	2.820833	0.402	12
C ₅	2.0089	15	2.32085	40	2.975286	0.544	21
C ₆	7.2347	21	4.10875	44	7.2385	0.404	8

In sample I₁, without compatibilizer, the population of individual particles was more than the core-shell ones. This fact was also predicted by Dynamic Interfacial Energy method when it predicted separated fully dispersed morphology for I₁ sample. However, it should be emphasized that the morphology of this ternary blend is complicated because it contains cavities, core-shell and individual particles simultaneously. Therefore, the Dynamic Interfacial Energy prediction method is just able to prognosticate dominant morphology. This statement is validated by the data of table 4 where number of individual particles (43) exceeds population of core-shell ones (14). In the sample I₂ where compatibilizer (SEBS-g-MA) was used, increase in core-shell particles was observed. In addition, population of the individual PET particles which have no compatibility with PP matrix decreased. This observation confirms formation of a strong interface between the blend components.

In sample I₂, shell thickness of core-shell particles became thinner while average diameter of core-shell and individual particles became bigger. Decrease in population of the individual particles and increase in number average diameter of composite particles signify that the PET particles situate on cores. Comparing I₁ and I₂ samples, it can be said that addition of rubbery phase leads to reduction in number of the individual PET particles. In the presence of the rubbery phase, these individual PET particles migrate toward core-shell ones and join to PET chains already exist in the core. This phenomenon results in production of core-shell particles with bigger core and thinner shell. This is why a reduction in shell thickness is observed in ta-

ble 4. Finally, sample I₃ showed a three morphologies consisting of the core-shell particles, individual particles and cavities where size of all of them increased in comparison with I₁ sample.

For samples C₁-C₃, SEBS percentage changed but the Dynamic Interfacial Energy method was not able to predict the real morphology. The method predicted core-shell morphology with SEBS as core and PET as shell, however, this prediction is not in agreement with thermodynamic axioms. From thermodynamic point of view, PP and PET are incompatible and their presence beside each other is impossible. By the addition of the rubbery phase, it was aimed to increase core-shell morphologies. Increasing rubbery phase ratio leads to increase in diameter of the composite particles. Population of individual PET particles also decreased which shows their immigration toward core of the composite particles. Increasing rubbery phase also is associated with shell diameter increase. This is why thermodynamic forces motivate added rubber chains to sit at interface of PET/PP phases to minimize their contact and thereby decreasing interfacial tension of the system. On the other hand, the average diameter of cavities increased which shows that some SEBS chains are jointed to already exist rubbery domains. This is why bigger cavities are appeared after dissolution in cyclohexane. For samples C₄-C₆, PET percentage was changed and both methods predicted the core-shell morphology. In these samples, by increasing the rigid phase, average diameter of cavities, the individual particles and the core-shell ones extremely increased, Figure 3. Generally, in all samples investigated in this study, it was found that several morphologies exist si

multaneously and the prediction methods used here are just able to predict dominant morphology. Among the all theories, Dynamic Interfacial Energy had the most successful predictions due to considering interfacial forces in the systems.

3.2. Mechanical properties

Table 5 summarizes the mechanical properties of the ternary blends prepared in this study. As a reference, the mechanical properties of PP matrix were measured.

The Young's modulus is controlled by volume fraction of the matrix and phases rigidity. The yield stress is controlled by several factors such as, volume fraction, average diameter and size distribution of the dispersed phases and also the interfacial adhesion between disperse and the matrix. Distribution of rubbery particles effectively increases the impact strength as well. [24-27]

Table 5.
Mechanical properties of various blends.

Sample code	Modulus (MPa)	Yield stress (MPa)	Impact strength (J/m)
Pure PP	1048.3±23.5	27.83±0.49	26.48±0.471
I ₁	337.36±42.3	19.89±1.14	52.85±0
I ₂	464.41±53.8	20.95±1.50	68.3±5.3
I ₃	414.68±31.1	17.76± 0.89	67.76±1.2
C ₁	998.29±50.8	21.46±0.43	81.66±4.43
C ₂	640.11±43.8	19.54±0.14	89.44±2.7
C ₃	276.11±35.1	17.93±0.18	104.04±4.72
C ₄	486.31±57.4	19.67±0.34	76.49±1.39
C ₅	1142.5±36.1	21.19±0.63	49.1±0
C ₆	1568.2±62.3	23.39±0.58	37.02±0.56

In samples I₁-I₃, only compatibilizer percentage changed. Sample I₁ which does not include compatibilizer showed the least properties in this group due to absence of good interfacial adhesion. On the other hand, it included the most cavities and the individual PET particles that affect properties greatly. For example, I₁ sample shows the least impact strength among I sample group which is caused by presence of a great number of individual PET particles. In sample I₂, compatibilizer and rubbery phase were used together. This sample showed most outstanding properties in this group [9]: The number of composite particles and their average diameter increased. Also, the number of the individual particles and population of cavities reduced which show compatibilizer establish an inter-

facial adhesion with matrix and cause the morphology to change to the core-shell one. These composite particles make strong interface with the matrix leading to significant enhance in impact strength. It can be also deduced that applying equal amount of SEBS and SEBS-g-MAH is a crucial factor in achieving high impact strength. This is why SEBS has higher molecular weight than SEBS-g-MAH and also better miscibility with PP chains which are influential factors in impact resistance improvement (miscibility factors (parameter B as a measure) for PP/SEBS and PP/SEBS-g-MAH are 1.1 and 0.86, respectively) [24]. In sample I₃ which just compatibilizer was used, the number of cavities increased and population of the individual particles and the number of composite particles decreased, as well. Although population of composite particles decreased and their size increased in I₃ sample comparing with I₁, its impact strength is higher. The determining factor here is population of individual PET particles. I₁ consists of 43 PET particles while I₃ has only 11 ones. Thus, it is obvious that there is an inverse correlation between number of individual PET particles and the impact strength of the system.

In samples C₁-C₃, rubbery phase amount changed and the results showed as rubbery phase amount increases, modulus and yield stress of the blends decreases. As mentioned above, the modulus is controlled by the volume fraction of matrix and the phase's rigidity. Increasing the amount of the rubbery phase led to rigidity decrease; therefore, the modulus decreased. Although yield stress is dependent on size and size distribution of dispersed particles and adhesion between phases, the softness and rigidness of phases are more important factors. So, C₂ and C₃ samples showed lower yield stress than C₁ sample due to increase in population of composite particles and decrease in number of the individual PET particles. Moreover, from C₁ toward C₃, impact strength is improved which is attributed to increase in population of core-shell particles.[28] Although average diameter of composite particles in this group is increased, the impact strength enhanced. Thus, it can be concluded that population of core-shell particle is more important factor in increasing impact strength than average diameter of them. Number of the individual PET particles in C₂ and C₃ samples is lower than C₁ which is another reason for impact strength improvement.

Increasing the PET content in C₄-C₆ samples is associated with increase in cavities size. Increase in dimension is also observed for the Individual PET particles and core-shell ones. These can be considered as reasons of reduction in impact strength of the samples in

this group. However, no regular trend in population of the cavities, the composite and the individual particles is seen. When the PET content reaches its maximum value (C_6), the poorest impact strength is observed. This is why the PET particles are not dispersed finely in the system and some aggregation are formed, Figure 3. Increase in average diameter of the individual PET particles is also attributed to this phenomenon. Modulus and yield stress of these samples increased by increase in population of individual particles and rigid phase amount.[29] SEM micrographs also show simultaneous presence of several morphologies in the blends of this group, however, both RIE and Dynamic Interfacial Energy predict core-shell morphology, Table 3. As a result, it can be said that such theories are not fully able to predict morphological state of the system and just estimate the dominant morphology in some cases.

According to the above-mentioned statements, weight ratio of SEBS to SEBS-g-MAH affects morphology and mechanical properties of the blends greatly. Compatibilizer percentage tailors the morphology through affecting interfacial forces. Finally, concerning the results of mechanical properties, optimum processing conditions for ternary PP/PET/SEBS blends were delineated as follows:

1. Die temperature: 260 °C
2. Screw speed: 130 rpm
3. Mixing sequence: PP and SEBS-g-MAH were first pre-blended and then extruded with PET and SEBS.
4. Composition: PP(wt%)= 63, PET(wt%)= 30, SEBS(wt%)= 3.5, SEBS-g-MA(wt%)=3.5

4. Conclusions

The ternary polymer blends based on PP/PET/SEBS investigated in this research showed very different morphologies compared with other ternary systems. The methods used for predicting the type of blend morphology were not fully successful and in some samples they were just able to predict the dominant morphology. SEM micrographs indicated that the blends included three morphologies of core-shell particles, individual particles and cavities. Mechanical inspection tests showed variation in mechanical properties with increasing SEBS-g-MAH content. It was shown that the compatibilizer amount causes changes in the dispersed phase morphology (i.e., type of morphology, average diameter and size distribution of dispersed phase, and interfacial adhesion). With increasing the rubbery phase, the core-shell morphology and the impact strength increased while the modulus de-

creased. Also, by increasing the amount of rigid phase, the number average diameter of cavities, the individual particles and the core-shells particles increased. In sum, the correlation between mechanical properties and morphology illustrated that the core-shell and the individual PET particles have positive and negative effects on impact strength, respectively. The rigid phase and the individual particles improved the modulus and decreased the impact strength, as well. By selecting deliberately weight ratio of ingredients, it is possible to produce various PP blends with improved modulus, impact strength and yield stress. Among all studied samples, the C_6 was the optimum one which showed higher modulus, acceptable yield stress and improved impact strength in compare to pure PP.

Acknowledgements

The authors would like to thank Abbas Farahani and Faezeh Rezaei (Mehr petrochemical) and Gholamhasan Heydarie for their assistance.

References

- [1] S. Y. Hobbs, M. E. J. Dekkers, V. H. Watkins, Effect of interfacial forces on polymer blend Morphologies, *Polymer* 29 (1988) 1598-1602.
- [2] T. S. Valera, A. T. Morita, N. R. Demarquette, Study of morphologies of PMMA/PP/PS ternary blends, *Macromolecules* 39 (2006) 2663-2675.
- [3] H. F. Guo, S. Packirisamy, N. V. Gvozdic, D. J. Meier, Prediction and manipulation of the phase morphologies of multiphase polymer blends: I. Ternary systems, *Polymer* 38 (1997) 785-794.
- [4] M. Hemmati, H. Nazokdast, H. S. Panahi, Study on morphology of ternary polymer blends. I. effects of melt viscosity and interfacial interaction, *J. Appl. Polym. Sci.* 82 (2001) 1129-1137.
- [5] J. Reignier, B. D. Favis, M.C. Heuzey, Factors influencing encapsulation behavior in composite drop-let-type polymer blends, *Polymer* 44 (2003) 49-59.
- [6] S. Shokoohi, A. Arefazar, A review on ternary immiscible polymer blends: morphology and effective parameters, *Polym. Adv. Technol.* 20 (2009) 433-447.
- [7] H. F. Guo, N.V. Gvozdic, D. J. Meier, Prediction and manipulation of the phase morphologies of multiphase polymer blends: II. Quaternary systems, *Polymer* 38 (1997) 4915-4923.
- [8] J. Reignier, B. D. Favis, Control of the subinclusion microstructure in HDPE/PS/PMMA ternary blends, *Macromolecules* 33 (2000) 6998-7008.

- [9] A. N. Wilkinson, M. L. Clemens, V. M. Harding, The effects of SEBS-g-maleic anhydride reaction on the morphology and properties of polypropylene/PA6/SEBS ternary blends, *Polymer* 45 (2004) 5239–5249.
- [10] I. Luzinov, C. Pagnouille, R. Jerome, Ternary polymer blend with core-shell dispersed phases: effect of the coreforming polymer on phase morphology and mechanical properties, *Polymer* 41 (2000) 7099–7109.
- [11] G. Jiang, H. Wu, S. Y. Guo, A study on compatibility and properties of POE/PS/SEBS ternary blends, *J. Macromol. Sci., Part B: Phys.* 46 (2007) 533–545.
- [12] E. Kuram, L. Sarac, B. Ozcelik, Mechanical, chemical, thermal, and rheological properties of recycled PA6/ABS binary and PA6/PA66/ABS ternary blends, *J. Appl. Polym. Sci.* 131 (2014) 40810.
- [13] Y. Han, F. Liu, Influence of blend composition on the mechanical properties and morphology of PC/ASA/SAN ternary blends, *Polym. Bull.* 62 (2009) 855–866.
- [14] N. Vranjes, V. Rek, Effect of EPDM on morphology, mechanical properties, crystallization behavior and viscoelastic properties of iPP+HDPE blends, *Macromol. Symp.* 258 (2007) 90-100.
- [15] O. M. Jazani, A. Arefazar, Evaluation of mechanical properties of polypropylene/polycarbonate/SEBS ternary polymer blends using taguchi experimental analysis, *J. Appl. Polym. Sci.* 116 (2010) 2312–2319.
- [16] Y. Zhou, B. Yin, L. Li, M. Yang, J. Feng, Characterization of PP/EPDM/HDPE ternary blends: the role of two EPDM with different viscosity and processing method, *Polym.-Plast. Technol. Eng.* 51 (2012) 983–990.
- [17] Y. Li, D. Wang, X. Xie, Influences of component ratio of minor phases and charge sequence on the morphology and mechanical properties of PP/PS/PA6 ternary blends, *Polym. Bull.* 66 (2011) 841–852.
- [18] B. Wang, Y. Yang, W. Guo, Effect of EVOH on the morphology, mechanical and barrier properties of PA6/POE-g-MAH/EVOH ternary blends, *Mater. Design.* 40 (2012) 185–189.
- [19] D. H. Park, W. N. Kim, Effects of compatibilizers and hydrolysis on the mechanical and rheological properties of polypropylene/EPDM/poly(lactic acid) ternary blends, *Macromol. Res.* 19 (2011) 105-112.
- [20] O. M. Jazani., A. Arefazar, S. H. Jafari, M. R. Peymanfar, M. R. Saeb, A. Talaei, SEBS-g-MAH as a reactive compatibilizer precursor for PP/PTT/SEBS ternary blends: morphology and mechanical properties, *Polym.-Plast. Technol. Eng.* 52 (2013) 206–212.
- [21] W. Zhang, J. Zhang, S. Chen, Effect of core-shell structured modifier ACR on ASA/SAN/ACR ternary blends. *J. Mater. Sci.* 47 (2012) 5041–5049.
- [22] M. M. Abolhasani, A. Arefazar, PET/EVA/PP ternary blends: an investigation of extended morphological properties. *J. Appl. Polym. Sci.* 112 (2009) 1716–1728.
- [23] N. Mostofi, H. Nazockdast, Study on morphology and viscoelastic properties of PP/PET/SEBS ternary blend and their fibers, *J. Appl. Polym. Sci.* 114 (2009) 3737–3743.
- [24] O. M. Jazani, A. Arefazar, A Study on the effects of SEBS-g-MAH on the phase morphology and mechanical properties of polypropylene/ polycarbonate/SEBS ternary polymer blends, *J. Appl. Polym. Sci.* 121 (2011) 2680–2687.
- [25] S. L. Bai, G. T. Wang, J. M. Hiver, G. Sell, Microstructures and mechanical properties of polypropylene/polyamide6/polyethelene-octene elastomer blends, *C. Polymer* 45 (2004) 3063-3071.
- [26] R. Gallego, D. García-López, Toughening of PA6/mEPDM blends by two methods of compounding, extruder and internal mixer: rheological, morphological and mechanical characterization, *Polym. Bull.* 60 (2008) 665-675.
- [27] A. S. Sarvestani, On the overall elastic moduli of composites with spherical coated fillers, *Int. J. Solids. Struct.* 40 (2003) 7553-7566.
- [28] J. Yu, P. Feng, H. Zhang, Effects of core-shell acrylate particles on impact properties of chlorinated polyethylene/polyvinyl chloride blends, *Polym. Eng. Sci.* 50 (2010) 295–301.
- [29] M. A. DeBolt, R. E. Robertson, Morphology of compatibilized ternary blends of polypropylene, nylon 66, and polystyrene, *J. Appl. Polym. Sci.* 46 (2006) 385-398.